

High-pressure synthesis, crystal structure, and properties of the first ternary hafniumborate β -HfB₂O₅

Johanna S. Knyrim, Hubert Huppertz*

Department Chemie und Biochemie, Ludwig-Maximilians-Universität München, Butenandtstrasse 5-13, D-81377 München, Germany

Received 13 October 2006; received in revised form 1 December 2006; accepted 4 December 2006

Available online 8 December 2006

Abstract

The first ternary hafniumborate β -HfB₂O₅ was synthesized under high-pressure and high-temperature conditions in a Walker-type multianvil apparatus at 7.5 GPa and 1100 °C. The monoclinic hafnium-diborate crystallizes with four formula units in the space group $P2_1/c$ with lattice parameters $a = 438.48(9)$, $b = 690.60(2)$, $c = 897.60(2)$ pm, and $\beta = 90.76(3)^\circ$. Due to the fact that high-pressure conditions favour the fourfold-coordination of boron, a structure is observed, which is built up exclusively from layers of BO₄ tetrahedra; between the layers, the hafnium ions are coordinated square-antiprismatically by eight oxygen atoms. A structural comparison of β -HfB₂O₅ with minerals of the gadolinite–homilite–hingganite–datolite family proved this compound to be the simplest structural variant in this structure type, known so far. Along with a structural discussion, temperature-programmed X-ray powder diffraction data are shown, demonstrating the metastable character of this compound.

© 2006 Elsevier Inc. All rights reserved.

Keywords: High-pressure; Multianvil; Crystal structure; Borate; Borosilicate; Gadolinite

1. Introduction

The parameter pressure represents a versatile tool for the exploration of new synthetic fields in solid state chemistry. Especially the multianvil technique has made it possible to synthesize reasonable amounts of new metastable compounds in areas of pressure, which were hitherto not accessible for conventional preparative chemistry. For example, the application of this method to the field of borates resulted in a variety of new polymorphs like β -MB₄O₇ ($M = \text{Ca, Zn, Hg}$) [1–3], χ -REBO₃ ($RE = \text{Dy, Er}$) [4], ν -DyBO₃ [5], γ -RE(BO₂)₃ ($RE = \text{La–Nd}$) [6], δ -La(BO₂)₃ [7], and compounds with new compositions such as RE₄B₆O₁₅ ($RE = \text{Dy, Ho}$) [8–10], α -RE₂B₄O₉ ($RE = \text{Sm–Ho}$) [11–13], β -RE₂B₄O₉ ($RE = \text{Dy, Gd}$) [14,15], and RE₃B₅O₁₂ ($RE = \text{Tm–Lu}$) [16]. RE₄B₆O₁₅ ($RE = \text{Dy, Ho}$) and α -RE₂B₄O₉ ($RE = \text{Sm–Ho}$) showed the structural feature of edge sharing BO₄ tetrahedra for the first time. Furthermore, it was possible to synthesize a

new non-centrosymmetric modification δ -BiB₃O₆ of the well-known nonlinear optical material bismuth triborate (BIBO) [17]. A qualitative powder second-harmonic generation (SHG) measurement of δ -BiB₃O₆ signaled a considerable SHG effect. Recently, we were able to synthesize a crystalline compound β -SnB₄O₇ by pressure-induced crystallization in a system, in which previously only glasses were known [18].

Based on these experiences, we intend to synthesize new borates in systems, where no defined crystalline materials can be obtained via conventional synthetic routes up to now. As far as we know, the ternary system Hf–B–O has got no amorphous or crystalline phase. In quaternary compounds, there exists only one borate Ni₅HfB₂O₁₀, which is built up from Ni/HfO₆ octahedra and BO₃ groups [19]. Our investigations into the ternary system Hf–B–O were now successful with the synthesis of the first hafnium-diborate β -HfB₂O₅. Due to the fact that this compound is a high-pressure phase, we labeled it with the Greek character “ β ”. Attempts to synthesize the ambient-pressure hafnium-diborate “ α -HfB₂O₅” are going on. In the following, the preparation, crystal structure, and thermal behavior of

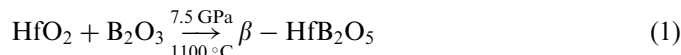
*Corresponding author. Fax: +49 89 2180 77806.

E-mail address: huh@cup.uni-muenchen.de (H. Huppertz).

β -HfB₂O₅ will be discussed. Furthermore, a comparison of β -HfB₂O₅ to analogs in the structural chemistry of borosilicates, beryllsilicates, borophosphates, and borates is given.

2. Experimental section

According to Eq. (1) β -HfB₂O₅ was prepared via a high-temperature/high-pressure synthesis from HfO₂ (Strem Chemicals, Newburyport, USA, 98%) and B₂O₃ (Strem Chemicals, Newburyport, USA, >99.9%)



A stoichiometric mixture of the oxides was ground and filled into a boron nitride crucible of an 18/11-assembly, which was compressed up to 7.5 GPa during 3 h, using a multianvil apparatus. Details of preparing the assembly can be found in Refs. [20–24]. The sample was heated to 1100 °C in 10 min, kept there for 5 min, and cooled down to 750 °C in 15 min. Afterwards, the sample was quenched to room temperature, followed by decompression over a period of 9 h. The recovered experimental octahedron was broken apart and the sample carefully separated from the surrounding boron nitride crucible yielding the white, crystalline compound β -HfB₂O₅. Analyzing the powder pattern of the reaction product, we were able to identify a small amount of unreacted HfO₂. The corresponding surplus boron oxide was not detectable in the powder XRD pattern (X-ray amorphous).

Systematic variations of the experimental conditions showed that β -HfB₂O₅ can be synthesized in the pressure range of 6–11 GPa applying temperatures of 800–1200 °C. The best results were obtained at the presented conditions of 7.5 GPa and 1100 °C.

3. Crystal structure analysis

Small single crystals of β -HfB₂O₅ were isolated by mechanical fragmentation and examined by Buerger precession against Laue photographs. Single crystal intensity data of β -HfB₂O₅ were measured with a Kappa-CCD-diffractometer (AXS-Nonius) [MoK_α radiation (71.073 pm)]. A numerical absorption correction (Habitus [25]) was applied to the data. According to the systematic extinctions $h0l$ with $l \neq 2n$, $0k0$ with $k \neq 2n$, and $00l$ with $l \neq 2n$, the monoclinic space group $P2_1/c$ (No. 14) was derived. The structure solution and parameter refinement (full-matrix least squares against F^2) were carried out via direct methods, using the SHELX-97 software suite [26]. Table 1 shows the details of the data collection and structure refinement. The positional parameters, anisotropic displacement parameters, interatomic distances, and interatomic angles are listed in Tables 2–5. Additional information of the crystal structure investigation may be obtained from the Fachinformationszentrum Karlsruhe, 76344 Eggenstein Leopoldshafen, Germany

Table 1
Crystal data and structure refinement of β -HfB₂O₅

Empirical formula	HfB ₂ O ₅
Molar mass (g mol ⁻¹)	280.11
Crystal system	Monoclinic
Space group	$P2_1/c$
<i>Lattice parameters from powder data</i>	
Radiation	CuK α_1 ($\lambda = 1.54051 \text{ \AA}$)
<i>a</i> (pm)	438.43(3)
<i>b</i> (pm)	690.48(6)
<i>c</i> (pm)	897.27(6)
β (deg)	90.76(1)
Volume (nm ³)	0.2716(1)
Single crystal diffractometer	Enraf–Nonius Kappa CCD
Radiation	MoK α ($\lambda = 0.71073 \text{ \AA}$)
<i>Single crystal data</i>	
<i>a</i> (pm)	438.48(9)
<i>b</i> (pm)	690.60(2)
<i>c</i> (pm)	897.60(2)
β (deg)	90.76(3)
Volume (nm ³)	0.2718(2)
Formula units per cell	$Z = 4$
Temperature (K)	293(2)
Calculated density (g cm ⁻³)	6.847
Crystal size (mm ³)	$0.044 \times 0.030 \times 0.022$
Absorption coefficient (mm ⁻¹)	38.24
<i>F</i> (000)	488
θ range (deg)	$3.1 \leq \theta \leq 35.0$
Range in <i>hkl</i>	$-7 \leq h \leq 6, -11 \leq k \leq 9, -14 \leq l \leq 14$
Total no. reflections	5887
Independent reflections	1186 ($R_{\text{int}} = 0.0372$)
Reflections with $I > 2\sigma(I)$	1144 ($R_{\sigma} = 0.0352$)
Data/parameters	1186/74
Absorption correction	Numerical (Habitus [25])
Transm. ratio (min/max)	0.270/0.497
Goodness-of-fit (F^2)	1.165
Final <i>R</i> indices ($I > 2\sigma(I)$)	$R_1 = 0.0201$ $wR_2 = 0.0498$
<i>R</i> indices (all data)	$R_1 = 0.0210$ $wR_2 = 0.0502$
Extinction coefficient	0.068(2)
Largest differ. peak, deepest hole (e \AA^{-3})	–2.432/2.143

Table 2
Atomic coordinates and equivalent isotropic displacement parameters U_{eq} (\AA^2) of β -HfB₂O₅ (space group $P2_1/c$; all Wyckoff site $4e$)

Atom	<i>x</i>	<i>y</i>	<i>Z</i>	U_{eq}
Hf	0.00132(3)	0.11281(2)	0.67087(2)	0.00420(8)
B1	0.5267(8)	0.2286(6)	0.4232(4)	0.0046(6)
B2	0.4652(9)	0.0871(7)	0.1655(4)	0.0039(6)
O1	0.7874(6)	0.0898(4)	0.1790(3)	0.0050(4)
O2	0.3297(6)	0.8950(3)	0.1502(3)	0.0051(5)
O3	0.3456(5)	0.2215(4)	0.0547(3)	0.0048(4)
O4	0.3039(5)	0.1555(4)	0.3078(3)	0.0043(4)
O5	0.7685(6)	0.0963(4)	0.4679(3)	0.0048(4)

U_{eq} is defined as one-third of the trace of the orthogonalized U_{ij} tensor.

Table 3
Anisotropic displacement parameters / \AA^2 of $\beta\text{-HfB}_2\text{O}_5$ (space group $P2_1/c$)

Atom	U_{11}	U_{22}	U_{33}	U_{12}	U_{13}	U_{23}
Hf	0.0050(2)	0.0039(2)	0.0038(2)	0.00006(3)	-0.00011(6)	0.00006(3)
B1	0.007(2)	0.003(2)	0.004(2)	0.000(2)	-0.001(2)	0.001(2)
B2	0.004(2)	0.005(2)	0.002(2)	-0.001(2)	0.000(2)	-0.001(2)
O1	0.004(2)	0.005(2)	0.006(2)	0.0014(8)	0.0001(8)	0.0001(8)
O2	0.006(2)	0.003(2)	0.006(2)	-0.0010(7)	0.0011(8)	-0.0011(7)
O3	0.0048(9)	0.004(2)	0.0054(9)	0.0017(8)	0.0005(7)	0.0013(8)
O4	0.004(2)	0.004(2)	0.0044(9)	-0.0015(8)	0.0001(7)	-0.0005(8)
O5	0.004(2)	0.004(2)	0.006(2)	-0.0009(7)	-0.0014(8)	0.0008(7)

Table 4
Interatomic distances /pm in $\beta\text{-HfB}_2\text{O}_5$ calculated with the single crystal lattice parameters

Hf–O5a	207.9(3)	B1–O5	145.2(5)
Hf–O1a	214.4(3)	B1–O2	147.0(4)
Hf–O5b	216.5(3)	B1–O3	147.2(4)
Hf–O3	217.2(2)	B1–O4	150.1(4)
Hf–O2	218.0(3)	\varnothing	$\varnothing = 147.4$
Hf–O1b	225.9(3)	B2–O1	141.7(5)
Hf–O4a	229.5(3)	B2–O3	145.3(5)
Hf–O4b	240.6(3)	B2–O2	145.9(5)
	$\varnothing = 221.2$	B2–O4	154.2(4)
		\varnothing	$\varnothing = 146.8$

Table 5
Interatomic angles (deg) in $\beta\text{-HfB}_2\text{O}_5$ calculated with the single crystal lattice parameters

O2–B1–O4	103.4(2)	O2–B2–O4	99.6(3)
O3–B1–O4	106.2(3)	O3–B2–O4	101.9(3)
O5–B1–O2	107.4(3)	O3–B2–O2	111.9(3)
O5–B1–O3	109.0(3)	O1–B2–O4	113.1(3)
O2–B1–O3	114.5(3)	O1–B2–O3	113.6(3)
O5–B1–O4	116.5(3)	O1–B2–O2	115.1(3)
	$\varnothing = 109.5$	\varnothing	$\varnothing = 109.5$

(fax: +49 7247 808 666; e-mail: crystdata@fiz-karlsruhe.de), on quoting the depository number CSD-417031.

The powder diffraction pattern was obtained in transmission geometry from a flat sample of $\beta\text{-HfB}_2\text{O}_5$, using a STOE STADI P powder diffractometer with monochromatized $\text{CuK}\alpha_1$ radiation. The diffraction pattern was indexed with the program ITO [27] on the basis of a monoclinic unit cell. Based on least-square fits of the powder data, the lattice parameters (Table 1) were calculated. The correct indexing of the patterns of $\beta\text{-HfB}_2\text{O}_5$ was confirmed by intensity calculations, taking the atomic positions from the refined crystal structure data [28]. The lattice parameters, determined from the powder data and single crystal data, fit well.

4. Results and discussion

Fig. 1 shows the crystal structure of $\beta\text{-HfB}_2\text{O}_5$ along [010] with layers of corner sharing BO_4 tetrahedra (Q^3),

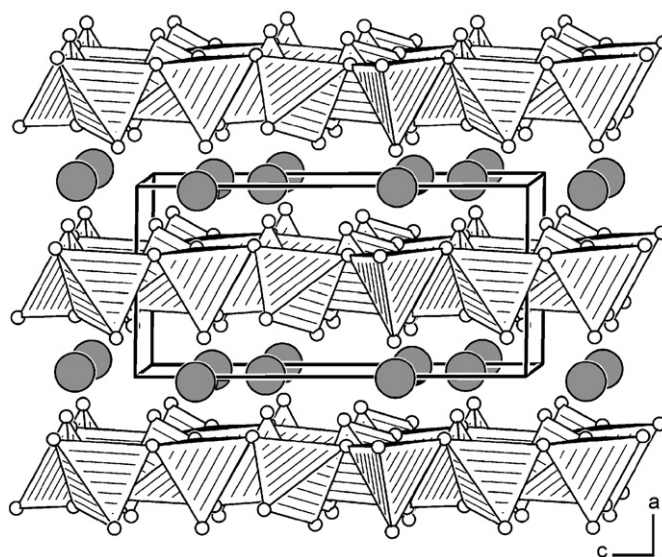


Fig. 1. Crystal structure of $\beta\text{-HfB}_2\text{O}_5$ (view along [010]), exhibiting layers of BO_4 tetrahedra and Hf^{4+} ions.

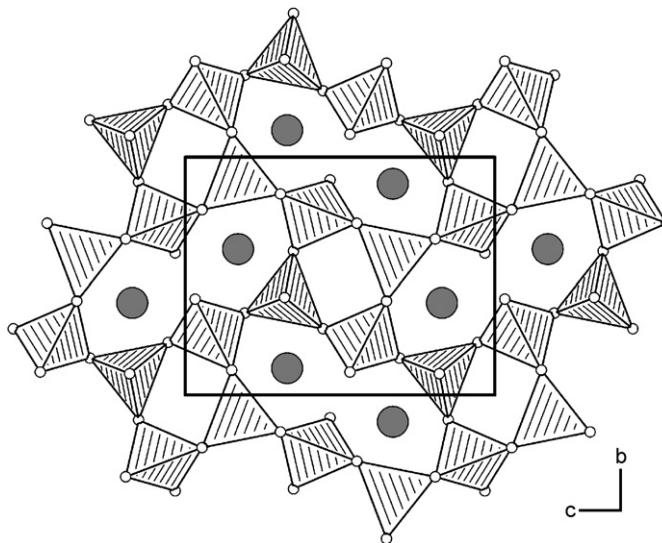


Fig. 2. View of the bc -plane in $\beta\text{-HfB}_2\text{O}_5$.

separated by Hf^{4+} ions. The layers are based on four- and eight-membered rings of BO_4 tetrahedra, extending in the bc -plane (Fig. 2). Fig. 3 gives a view of the Hf^{4+} ions,

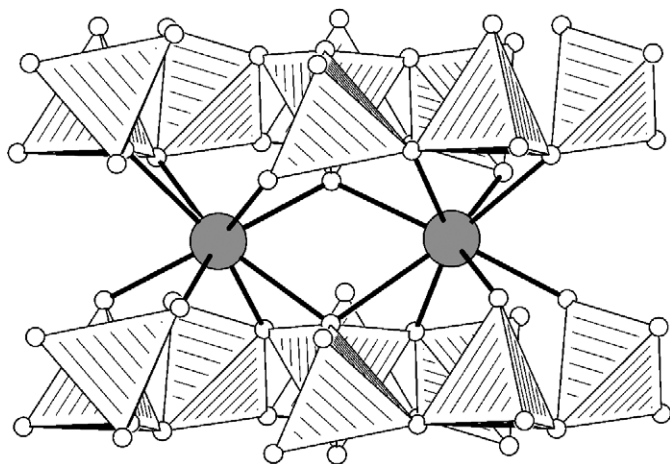


Fig. 3. Distorted square-antiprismatic coordination of Hf^{4+} in $\beta\text{-HfB}_2\text{O}_5$.

Table 6
Charge distribution in $\beta\text{-HfB}_2\text{O}_5$ calculated with the bond-length/bond-strength concept (ΣV) [34,35] and the CHARDI concept (ΣQ) [36]

	Hf	B1	B2	O1	O2	O3	O4	O5
ΣV	3.78	3.03	3.10	-1.84	-2.05	-2.07	-1.97	-1.98
ΣQ	4.01	2.98	3.02	-1.94	-2.08	-2.10	-1.81	-2.08

which are positioned between these sheets and coordinated by eight oxygen atoms in a distorted square-antiprismatic way. In the two crystallographically distinguishable BO_4 tetrahedra the B–O distances vary between 142 and 154 pm with a mean value of 147.1 pm, which corresponds well with the known average value of 147.6 pm for boron–oxygen bonds in BO_4 tetrahedra [29,30]. The angles O–B–O range between 99.6° and 116.5° with a mean value of 109.5° . The application of Liebau’s nomenclature for silicates [31] to the arrangement of tetrahedra in the structure of $\beta\text{-HfB}_2\text{O}_5$ leads to the formula $\text{Hf}\{\text{uB}, 1_\infty^2\}[\text{B}_2\text{O}_5]$, representing an unbranched “Vierer” single layer. The Hf–O distances range from 208 to 241 pm with a mean value of 221.2 pm, which is slightly higher than the average Hf–O distance of 218.8 pm in HfSiO_4 [32] or $\beta\text{-HfMo}_2\text{O}_8$ [33]. The calculation of bond-valence sums for $\beta\text{-HfB}_2\text{O}_5$ with the help of bond-length/bond-strength (ΣV) [34,35] and CHARDI (ΣQ) [36] concepts confirm the formal ionic charges of the atoms, acquired by the X-ray structure analysis. Table 6 shows the values for each atom. Furthermore, we calculated the Madelung part of lattice energy (MAPLE) values [37–39] for $\beta\text{-HfB}_2\text{O}_5$ in order to compare them with MAPLE values of the binary components HfO_2 and the high-pressure modification $\text{B}_2\text{O}_3\text{-II}$. As its basis serves the additive potential of the MAPLE-values, by which it is possible to calculate hypothetical values for $\beta\text{-HfB}_2\text{O}_5$, starting from the binary oxides. For $\beta\text{-HfB}_2\text{O}_5$ we obtained a value of 34,626 kJ/mol in comparison to 34,729 kJ/mol (deviation: 0.3%), starting

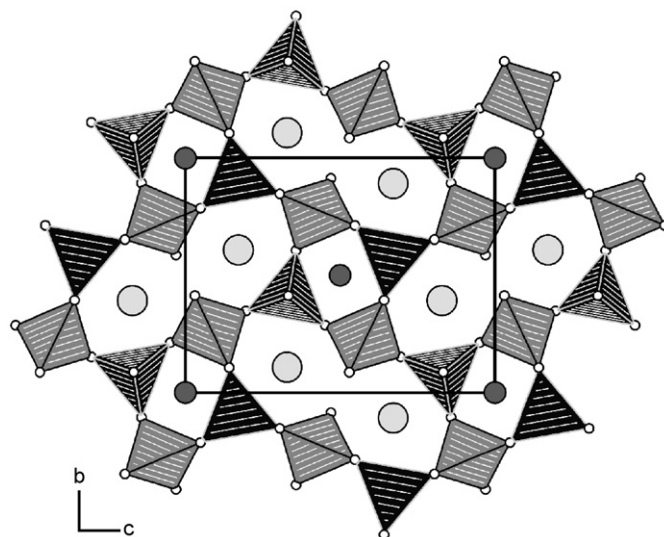


Fig. 4. Crystal structure of gadolinite-(Y) viewed along [100]. Y^{3+} ions are shown as light gray spheres and Fe^{2+} as dark gray spheres. Gray tetrahedra represent SiO_4 and black tetrahedra BeO_4 groups.

from the binary oxides [$1 \times \text{HfO}_2$ (12,791 kJ/mol) + $1 \times \text{B}_2\text{O}_3\text{-II}$ (21,938 kJ/mol)].

The arrangement of the BO_4 tetrahedra in $\beta\text{-HfB}_2\text{O}_5$, exhibiting four- and eight-membered rings, reminds of the crystal structure of apophyllite $\text{KCa}_4[\text{Si}_4\text{O}_{10}]_2(\text{F},\text{OH}) \cdot 8\text{H}_2\text{O}$ [40]. This structure is also composed of layers of rings (SiO_4 tetrahedra) with the same ring-sizes, but the tetrahedral sequence inside the rings shows a different topology. A closer comparison leads to minerals of the gadolinite group, in which the topology of the tetrahedra is identical to the arrangement in $\beta\text{-HfB}_2\text{O}_5$. Fig. 4 shows the structure of gadolinite-(Y) $\text{Y}_2\text{Be}_2\text{FeSi}_2\text{O}_8\text{O}_2$ [41,42], exhibiting the similar arrangement of tetrahedra as found in $\beta\text{-HfB}_2\text{O}_5$. The difference is that the tetrahedra in gadolinite-(Y) are centered alternately by beryllium (black polyhedra) and silicon atoms (gray polyhedra). Additionally, iron atoms are positioned in the origin of the unit cell beneath and above the four membered rings.

Several minerals and synthetic compounds belong to the gadolinite group (space group $P2_1/c$), which can be represented by the general chemical formula $A_2Z_2X\text{Si}_2\text{O}_8(\text{O},\text{OH})_2$. Demartin et al. [43] reviewed several members of this family, including datolite $\text{CaBSiO}_4(\text{OH})$ [44–47] (Fig. 5), homilite $\text{Ca}_2\text{B}_2\text{FeSi}_2\text{O}_8\text{O}_2$ [48], hingganite-(Y) $\text{Y}_2\text{Be}_2\text{Si}_2\text{O}_8(\text{OH})_2$ [43], hingganite-(Yb) $\text{Yb}_2\text{Be}_2\text{Si}_2\text{O}_8(\text{OH})_2$ [49], minasgeraisite-(Y) $\text{Y}_2\text{Be}_2\text{CaSi}_2\text{O}_8(\text{OH})_2$ [50], and synthetic compounds like calcybeborosilelite-(Y) $(\text{Y},\text{Ca})_2(\text{B},\text{Be})_2\text{Si}_2\text{O}_8(\text{OH},\text{O})_2$ [51], calciogadolinite $\text{CaYBe}_2\text{FeSi}_2\text{O}_8\text{O}_2$ [52–54], and $\text{NiYb}_2\text{Be}_2\text{Si}_2\text{O}_{10}$ [55]. A common feature of all these compounds is the fact that at least half of the tetrahedral positions are occupied by silicon atoms. This is also expressed by the general formula $A_2Z_2X\text{Si}_2\text{O}_8(\text{O},\text{OH})_2$, in which Z stands for the atoms, that occupy the second half of tetrahedral positions. To include the replacement of silicon at the tetrahedral position against

other suitable atoms, we modified the general formula of Demartin et al. to $A_2Z_2XT_2O_8(O,OH)_2$. This way, compounds like herderite $Ca_2Be_2P_2O_8(OH)_2$ [56], bakerite $Ca_4B_5Si_3O_{15}(OH)_5$ [57], $CuTm_2(B_2O_5)_2$ [58], $NiHo_2(B_2O_5)_2$ [59] and β -hafnium-diborate $HfB_2O_5 \rightarrow Hf_2B_2B_2O_8O_2$ (this work) can be included into the systematic representation of this structure family. Table 7 gives a survey of the different compositions including cell parameters, volume, c/a -, b/a -ratio, density, and an assignment of the cations to their positions.

In the general formula $A_2Z_2XT_2O_8(O,OH)_2$ the A site is occupied by rare earth (RE) or calcium ions, Z includes boron or beryllium, the T site contains silicon, phosphorous, or boron, and the X site can be filled with Fe^{2+} , Ni^{2+} ,

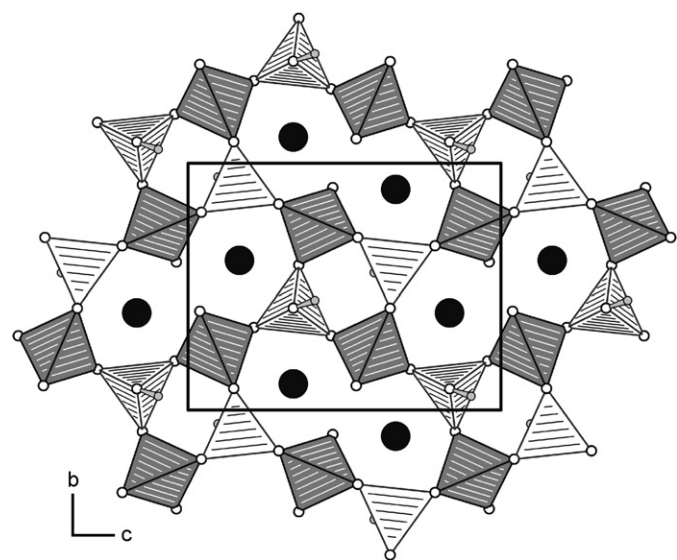


Fig. 5. Projection of the structure of datolite $Ca(BSiO_4)OH$ in the bc -plane. Ca^{2+} ions are shown as black spheres and protons as gray spheres. Light polyhedra represent BO_3OH groups and gray polyhedra SiO_4 groups.

and Cu^{2+} ions or remains empty. The occupation with Ca^{2+} or Fe^{3+} , as listed in the examples calciogadolinite and minasgeraisite-(Y), seems to be most doubtful. Often, vacancies on the X site are charge balanced by the substitution of oxygen ions for hydroxyl ions, e.g. $RE_2Be_2FeSi_2O_8O_2$ (gadolinite) $\rightarrow RE_2Be_2Si_2O_8(OH)_2$ (hingganite). Burt described this substitution giving an operator $(OH)_2(FeO_2)_{-1}$, not involving real vacancies but favored on crystal-chemical reasons for balancing the charge variation [60]. Furthermore, the replacement of RE and Be by Ca and B , respectively, leads to the second operator $CaB(REBe)_{-1}$. Starting with gadolinite $RE_2Be_2FeSi_2O_8O_2$, the operator $(OH)_2(FeO_2)_{-1}$ leads to the end member hingganite, $CaB(REBe)_{-1}$ to the final compound homilite $Ca_2B_2FeSi_2O_8O_2$, and if both operators act together, datolite $Ca_2B_2Si_2O_8(OH)_2$ is the final end member of these substitutions. Fig. 5 shows the structure of datolite built up from BO_3OH (light tetrahedra) and SiO_4 tetrahedra (gray polyhedra), in which the X site is empty. For compensation, the hydrogen atoms of the hydroxyl groups point to the X site. A detailed discussion of further variants of substitution can be found in Ref. [43]. Also other variants can be realized by substitutions on the T site, e.g., herderite $Ca_2Be_2P_2O_8(OH)_2$, which is built up from sheets of corner sharing PO_4 and BeO_3OH tetrahedra (alternating) [56]. Even a total occupation of the tetrahedral positions by boron atoms was possible in the synthetic compounds $CuTm_2(B_2O_5)_2$ [58] and $NiHo_2(B_2O_5)_2$ [59].

In this structure family, β -hafnium-diborate represents the first ternary compound with Hf^{4+} on the A site, boron on the Z and T sites, and an empty position X corresponding to " $Hf_2B_2B_2O_8O_2$ " $\rightarrow HfB_2O_5$. Hydrogen was excluded by IR spectroscopic investigations, in which no absorptions of hydroxyl groups or water could be found. So, β - HfB_2O_5 can be considered as the simplest structural variant of all compounds belonging to the gadolinite family. Table 7 illustrates, that the unit cell of

Table 7
Survey of different compositions

Name	Formula	A	Z	T	X	a (pm)	b (pm)	c (pm)	β (deg)	c/a	b/a	V (\AA^3)	ρ (g cm^{-3})	Ref.
Gadolinite-(Y)	$Y_2Be_2FeSi_2O_8O_2$	Y	Be	Si	Fe^{2+}	476.8 (1)	756.5 (2)	1000.0 (2)	90.31 (2)	2.097	1.586	360.7 (1)	4.307	[41,42]
Datolite	$Ca_2B_2Si_2O_8(OH)_2$	Ca	B	Si	Vac.	483.2 (4)	760.8 (4)	963.6 (8)	90.40 (7)	1.994	1.575	354.2	2.999	[44–47]
Homilite	$Ca_2B_2FeSi_2O_8O_2$	Ca	B	Si	Fe^{2+}	477.6 (1)	762.1 (2)	978.6 (2)	90.61 (2)	2.049	1.596	356.2 (1)	3.451	[48]
Hingganite-(Yb)	$Yb_2Be_2Si_2O_8(OH)_2$	Yb	Be	Si	Vac.	474.0 (2)	760.7 (3)	988.8 (5)	90.45 (4)	2.086	1.605	356.5	5.424	[49]
Hingganite-(Y)	$Y_2Be_2Si_2O_8(OH)_2$	Y	Be	Si	Vac.	474.4 (7)	757.1 (8)	981.1 (11)	90.26 (2)	2.068	1.596	352.4 (8)	3.901	[43]
Minasgeraisite-(Y) ^b	$Y_2Be_2CaSi_2O_8(OH)_2$	Y	Be	Si	Ca^{2+}	470.2 (1)	756.2 (1)	983.3 (2)	90.46 (6)	2.091	1.608	349.6 (2)	4.313	[50]
Bakerite	$Ca_4B_5Si_3O_{15}(OH)_5$	Ca	B	Si	Vac.	480.0 (1)	757.9 (1)	954.3 (1)	90.44 (1)	1.988	1.579	347.2	2.982	[57]
Calcybeborosilelite-(Y)	$(Y,Ca)_2(B,Be)_2Si_2O_8(OH,O)_2$	Y + Ca	B, Be	Si	Vac. ^a	476.6 (2)	760.0 (2)	984.6 (4)	90.11 (3)	2.066	1.595	356.6	3.408	[51]
Calcioadolinite ^b	$CaYBe_2FeSi_2O_8O_2$	Y + Ca	Be	Si	Fe^{3+}	469.6 (1)	756.6 (2)	998.8 (2)	90.1 (2)	2.127	1.611	354.0 (2)	3.931	[52–54]
	$NiYb_2Be_2Si_2O_{10}$	Yb	Be	Si	Ni^{2+}	466.4 (4)	738.5 (4)	986.6 (8)	90.02	2.115	1.583	339.8	6.244	[55]
Herderite	$Ca_2Be_2P_2O_8(OH)_2$	Ca	Be	P	Vac.	480.4 (1)	766.1 (1)	978.9 (2)	90.02 (1)	2.038	1.595	360.3	2.969	[56]
	$CuTm_2(B_2O_5)_2$	Tm	B	B	Cu^{2+}	452.18 (7)	720.0 (2)	929.2 (5)	90.16 (5)	2.055	1.593	302.5 (2)	6.638	[58]
	$NiHo_2(B_2O_5)_2$	Ho	B	B	Ni^{2+}	451.0 (4)	724.8 (3)	938.8 (6)	91.39	2.082	1.607	306.8 (3)	6.406	[59]
β -Hafnium-diborate	$HfB_2O_5 \rightarrow Hf_2B_2B_2O_8O_2$	Hf	B	B	Vac.	438.48 (9)	690.60 (2)	897.60 (2)	90.76 (3)	2.047	1.575	271.8 (2)	6.847	This work
β -Zirconium-diborate	$ZrB_2O_5 \rightarrow Zr_2B_2B_2O_8O_2$	Zr	B	B	Vac.	439.04 (9)	691.2 (1)	896.8 (1)	90.96 (3)	2.043	1.574	272.1 (2)	4.708	[61]

Vac. = vacant.

^aVac. = nearly vacant.

^b = doubtful, redetermination of the crystal structure would be useful.

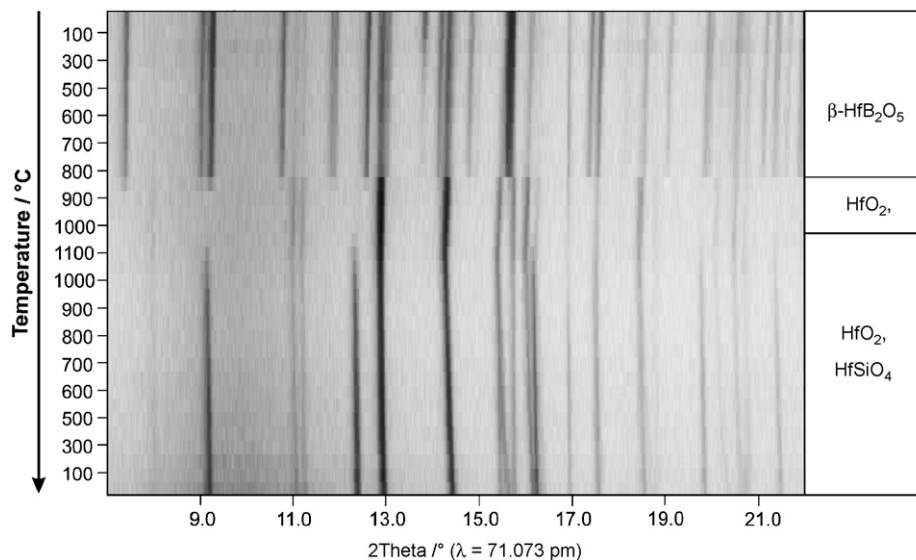


Fig. 6. Temperature-programmed X-ray powder patterns, showing the decomposition of β -HfB₂O₅.

β -HfB₂O₅ has the lowest extension ($V = 271.8(2) \text{ \AA}^3$) and the highest density (6.847 g/cm^3) of all compounds given, while the c/a and b/a ratios correspond to the values of the other phases. This is caused by the fact that β -HfB₂O₅ is a dense metastable high-pressure phase.

Recently, our attempts to synthesize the isotopic zirconium compound β -ZrB₂O₅, applying similar reaction conditions, were also successful [61]. It crystallizes with nearly identical lattice parameters ($a = 439.04(9)$, $b = 691.2(1)$, $c = 896.8(1)$ pm, and $\beta = 90.96(3)^\circ$; Table 7). In analogy to β -HfB₂O₅, the zirconium phase is the first defined ternary compound in the system Zr–B–O.

4.1. Thermal behavior

Temperature-programmed X-ray powder diffraction experiments were performed on a STOE Stadi P powder diffractometer (MoK α_1) with a computer controlled STOE furnace: The sample was enclosed in a quartz capillary and heated from room temperature to 500 °C in 100 °C steps and from 500 to 1100 °C in 50 °C steps. Afterwards, the sample was cooled down to 500 °C in 50 °C steps, and below 500 °C in 100 °C steps. At each temperature a diffraction pattern was recorded over the angular range $7^\circ \leq 2\theta \leq 22^\circ$. Fig. 6 illustrates the temperature-programmed X-ray powder diffraction patterns of β -HfB₂O₅, showing a decomposition of the high-pressure phase into HfO₂ and supposed B₂O₃ after successive heating to 800–850 °C. Heating above 1000 °C caused a reaction with the quartz capillary, leading to HfSiO₄ [32].

5. Conclusions

Using high-pressure/high-temperature conditions it was possible to synthesize the first ternary compound β -HfB₂O₅ in the system Hf–B–O. In contrast to normal pressure

investigations in borate systems, which often lead to amorphous compounds (glasses), pressure seems to favour the formation of crystalline compounds in borate chemistry. This is supported by a recently synthesized high-pressure tin borate β -SnB₄O₇, representing the first crystalline compound in the system Sn–B–O [18]. The mentioned phase β -ZrB₂O₅ is the third compound, where the high-pressure/high-temperature strategy was successfully applied. Therefore, we hope to have access to several other systems in borate chemistry, where no compounds exist until now. Due to high-pressure conditions, new structural features and interesting physical properties may be expected.

Acknowledgments

We thank Dr. Peter Mayer for collecting the single-crystal data, Thomas Miller for the in situ powder diffraction measurements, and Christian Minke (LMU München) for technical support. Special thanks go to Prof. Dr. W. Schnick (LMU München) for his continuous support of these investigations. This work was financially supported by the Deutsche Forschungsgemeinschaft (HU 966/2-2) and the European Science Foundation within the COST D30 network (D30/003/03).

References

- [1] H. Huppertz, Z. Naturforsch. B 58 (2003) 257.
- [2] H. Huppertz, G. Heymann, Solid State Sci. 5 (2003) 281.
- [3] H. Emme, M. Weil, H. Huppertz, Z. Naturforsch. B 60 (2005) 815.
- [4] H. Huppertz, B. von der Eltz, R.-D. Hoffmann, H. Piotrowski, J. Solid State Chem. 166 (2002) 203.
- [5] H. Emme, H. Huppertz, Acta Crystallogr. C 60 (2004) i117.
- [6] H. Emme, C. Despotopoulou, H. Huppertz, Z. Anorg. Allg. Chem. 630 (2004) 2450.
- [7] G. Heymann, T. Soltner, H. Huppertz, Solid State Sci. 8 (2006) 821.

- [8] H. Huppertz, B. von der Eltz, *J. Am. Chem. Soc.* 124 (2002) 9376.
- [9] H. Huppertz, *Z. Naturforsch. B* 58 (2003) 278.
- [10] H. Huppertz, H. Emme, *J. Phys.: Condens. Matter* 16 (2004) S1283.
- [11] H. Emme, H. Huppertz, *Z. Anorg. Allg. Chem.* 628 (2002) 2165.
- [12] H. Emme, H. Huppertz, *Chem. Eur. J.* 9 (2003) 3623.
- [13] H. Emme, H. Huppertz, *Acta Crystallogr. C* 61 (2005) i29.
- [14] H. Huppertz, S. Altmannshofer, G. Heymann, *J. Solid State Chem.* 170 (2003) 320.
- [15] H. Emme, H. Huppertz, *Acta Crystallogr. C* 61 (2005) i23.
- [16] H. Emme, M. Valldor, R. Pöttgen, H. Huppertz, *Chem. Mater.* 17 (2005) 2707.
- [17] J.S. Knyrim, P. Becker, D. Johrendt, H. Huppertz, *Angew. Chem.* 118 (2006) 8419; *J.S. Knyrim, P. Becker, D. Johrendt, H. Huppertz, Angew. Chem. Int. Ed. Engl.* 45 (2006) 8239.
- [18] J.S. Knyrim, F.M. Schappacher, R. Pöttgen, J. Schmedt auf der Günne, D. Johrendt, H. Huppertz, *Chem. Mater.* 19 (2007) in press.
- [19] K. Bluhm, H. Müller-Buschbaum, *Z. Anorg. Allg. Chem.* 575 (1989) 26.
- [20] D. Walker, M.A. Carpenter, C.M. Hitch, *Am. Mineral.* 75 (1990) 1020.
- [21] D. Walker, *Am. Mineral.* 76 (1991) 1092.
- [22] H. Huppertz, *Z. Kristallogr.* 219 (2004) 330.
- [23] D.C. Rubie, *Phase Transitions* 68 (1999) 431.
- [24] N. Kawai, S. Endo, *Rev. Sci. Instrum.* 8 (1970) 1178.
- [25] W. Herrendorf, H. Bärnighausen, University of Karlsruhe, Giessen, Germany, 1993/1997.
- [26] G.M. Sheldrick, University of Göttingen, Germany, 1997.
- [27] J.W. Visser, *J. Appl. Crystallogr.* 2 (1969) 89.
- [28] STOE & CIE GmbH, Darmstadt, Germany, 1998.
- [29] E. Zobetz, *Z. Kristallogr.* 191 (1990) 45.
- [30] F.C. Hawthorne, P.C. Burns, J.D. Grice, The crystal chemistry of boron, in: second ed. E.S. Grew, L.M. Anovitz, (Eds.), *Boron: Mineralogy, Petrology and Geochemistry*, vol. 33, Mineralogical Society of America, Washington, 1996, p. 41.
- [31] F. Liebau, *Structural Chemistry of Silicates*, Springer, Berlin, 1985.
- [32] J.A. Speer, B.J. Cooper, *Am. Mineral.* 67 (1982) 804.
- [33] S.N. Achary, G.D. Mukherjee, A.K. Tyagi, B.K. Godwal, *Phys. Rev. B* 66 (2002) 184106.
- [34] I.D. Brown, D. Altermatt, *Acta Crystallogr. B* 41 (1985) 244.
- [35] N.E. Brese, M. O'Keeffe, *Acta Crystallogr. B* 47 (1991) 192.
- [36] R. Hoppe, S. Voigt, H. Glaum, J. Kissel, H.P. Müller, K.J. Bernet, *J. Less-Common Met.* 156 (1989) 105.
- [37] R. Hoppe, *Angew. Chem.* 78 (1966) 52; *R. Hoppe, Angew. Chem. Int. Ed. Engl.* 5 (1966) 96.
- [38] R. Hoppe, *Angew. Chem.* 82 (1970) 7; *R. Hoppe, Angew. Chem. Int. Ed. Engl.* 9 (1970) 25.
- [39] R. Hübenthal, Version 4 ed., University of Giessen, Germany, 1993.
- [40] H. Bartl, G. Pfeifer, *Neues Jahrb. Mineral. Monatsh.* 58 (1976).
- [41] P.V. Pavlov, N.V. Belov, *Sov. Phys. Crystallogr.* 4 (1959) 300.
- [42] R. Miyawaki, I. Nakai, K. Nagashima, *Am. Mineral.* 69 (1984) 948.
- [43] F. Demartin, A. Minaglia, C.M. Gramaccioli, *Can. Mineral.* 39 (2001) 1105.
- [44] T. Ito, H. Mori, *Acta Crystallogr.* 6 (1953) 24.
- [45] F.F. Foit Jr., M.W. Phillips, G.V. Gibbs, *Am. Mineral.* 58 (1973) 909.
- [46] A.K. Pant, D.W.J. Cruickshank, *Z. Kristallogr.* 125 (1967) 286.
- [47] M. Watanabe, K. Nagashima, *Acta Crystallogr. B* 28 (1972) 326.
- [48] R. Miyawaki, I. Nakai, K. Nagashima, *Acta Crystallogr.* 41 (1985) 13.
- [49] A.B. Voloshin, I.A. Pakhomovskii, I.P. Menshikov, *Dokl. Akad. Nauk USSR* 270 (1983) 1188.
- [50] E. Foord, R.V. Gaines, J.G. Crock, W.B. Simmons Jr., C.P. Barbosa, *Am. Mineral.* 71 (1986) 603.
- [51] R.K. Rastsvetaeva, D.Y. Pushcharovskii, I.V. Pekov, A.V. Voloshin, *Kristallografiya* 42 (1996) 217.
- [52] T. Nakai, *Bull. Chem. Soc. Jpn.* 13 (1938) 591.
- [53] J. Ito, *Am. Mineral.* 52 (1967) 1523.
- [54] J. Ito, S.S. Hafner, *Am. Mineral.* 59 (1974) 700.
- [55] F.F. Foit Jr., G.V. Gibbs, *Z. Kristallogr. Kristallgeom. Kristallphys. Kristallchem.* 141 (1975) 375.
- [56] G.A. Lager, G.V. Gibbs, *Am. Mineral.* 59 (1974) 919.
- [57] N. Perchiazzi, A.F. Gualtieri, S. Merlino, A.R. Kampf, *Am. Mineral.* 89 (2004) 767.
- [58] J. Schaefer, K. Bluhm, *Z. Naturforsch. B* 50 (1994) 630.
- [59] K. Bluhm, A. Wiesch, *Z. Naturforsch. B* 51 (1995) 677.
- [60] D.M. Burt, Compositional and phase relations among rare earth element minerals, in: B.R. Lipin, G.A. McKay (Eds.), *Geochemistry and Mineralogy of Rare Earth Elements*, vol. 21, Mineralogical Society of America, Washington, Rev. Mineral. (1989) 259.
- [61] J. S. Knyrim, H. Huppertz, unpublished results, 2006.